Molecular Crystals and Liquid Crystals Science and Technology. Section A. Molecular Crystals and Liquid Crystals

Publication details, including instructions for authors and subscription information:
http://www.tandfonline.com/loi/gmcl19

LC-Conductivity and Cell Parameters; Their Influence on Twisted Nematic and Supertwisted Nematic Liquid Crystal Displays

H. Seiberle [a] & M. Schadt [a]

[a] Roche Liquid Crystal Research and Development, F. Hoffmann-La Roche Ltd, Dept. RLCR, 4002, Basel, Switzerland

Version of record first published: 04 Oct 2006.

To cite this article: H. Seiberle & M. Schadt (1994): LC-Conductivity and Cell Parameters; Their Influence on Twisted Nematic and Supertwisted Nematic Liquid Crystal Displays, Molecular Crystals and Liquid Crystals Science and Technology. Section A. Molecular Crystals and Liquid Crystals, 239:1, 229-244

To link to this article: http://dx.doi.org/10.1080/10587259408047185

Mol. Cryst. Liq. Cryst., 1994, Vol. 239, pp. 229–244
Reprints available directly from the publisher
Photocopying permitted by license only

Printed in the United States of America

LC-Conductivity and Cell Parameters; Their Influence on Twisted Nematic and Supertwisted Nematic Liquid Crystal Displays

H. SEIBERLE and M. SCHADT

Roche Liquid Crystal Research and Development, F. Hoffmann-La Roche Ltd, Dept. RLCR, 4002 Basel, Switzerland

(Received March 1, 1993; in final form June 1, 1993)

Charge transport mechanisms and the complex impedance of liquid crystal displays are shown to have a strong effect on the electro-optical performance of passive and active matrix addressed twisted nematic and supertwisted nematic LCDs. The static and dynamic dependence of the LCD-performance on liquid crystal material parameters, especially on resistivity, LCD cell gap, surface aligning layers and electrode conductivity are shown. From the proposed model follow the conditions to achieve frequency independent LCD-operation.

1. INTRODUCTION

When optimizing the performance of high information content, passive and active matrix addressed twisted nematic (TN) and supertwisted nematic (STN) liquid crystal displays (LCDs) with respect to multiplexibility, grey scale, contrast and cross-talk, the dynamics of the transport properties of charge carriers in the liquid crystal (LC) layer were so far hardly taken into account. Except for thin film transistor (TFT) addressed TN-LCDs, where a crucial prerequisite for high charge retention are highly resistive LC-materials, LC-resistivity is usually not an issue in the design of LCDs. However, negligence of this important and complex LC-material parameter may lead to a far from optimal electro-optical performance of high information content STN- and TFT-TN-LCDs.

The frequency dependent impedance $Z_p(\omega)$ of each LCD picture element (pixel) is not only determined by the complex impedance Z_{LC} of the liquid crystal layer,[1] but also by the cell geometry and by the passive materials used on the LCD-substrates. This has been partly presented at SID 92.[2] As a consequence of $Z_p(\omega)$, the externally applied voltage need not be identical with the actual, frequency dependent voltage V_{LC} across the LC-layer which determines the director defor-

mation and thus the electro-optical appearance of the LCD. Moreover, not only field-induced, but also current-induced nematic director deformations may occur in the LC-layer, thus further complicating matters.

Thanks to modern, active matrix addressable LC-materials which exhibit orders of magnitude smaller residual ionic impurities than conventional nematic LCs it has become possible to investigate the charge carrier transport in LC-layers and its influence on the electro-optical performance of LCDs over many orders of magnitude by selectively doping highly resistive LCs with ionic impurities. In the following we present a model which correlates the dynamics of charge carrier transport in LC-layers with the frequency- and time dependence of the optical threshold voltage, cross-talk and charge retention of TN-, TFT-TN- and STN-LCDs. An equivalent circuit which is consistent with the model in the nematic and in the isotropic phase of liquid crystals is presented. A single charge carrier transport mechanism is shown to be sufficient to describe the frequency—and the time dependence of the electro-optical performance of LCDs on conductivity and display parameters.

2. EXPERIMENTAL

The bulk resistivity ρ_{LC} and the dielectric constants $\varepsilon_\perp$ and $\varepsilon_\parallel$ of the liquid crystals were determined from the complex impedance of a parallel plate capacitor comprising the magnetic field-aligned LC as a dielectric.[1] Because of likely ionic contamination of the LC-layer in the display via the LCD substrates, the effective LC-resistivity $\rho_{LCD} \leq \rho_{LC}$ was determined in situ in the display.

In current-transient experiments bipolar voltages with amplitudes between 0.2 . . . 10 volts were used to drive the LCDs; the corresponding currents were determined with a Keithley picoammeter, model 610C. From the open circuit time dependence of the voltage decay across the LCD upon application of a single, 64 μs voltage pulse, the holding ratio HR[3] of the LCD picture element (pixel) was determined. Depending on the experiment, up to two hundred milliseconds were chosen as a time frame. To correlate in the experiments the actual voltage across a pixel with the applied voltage the optical transmission of the LCD was monitored simultaneously.

The experiments were performed in commercially available test LCDs (Optrex, 0.5×0.5 cm^2 pixel area) as well as in LCDs made in our laboratories. In the latter the electrode gap d and the thickness δ of the aligning layers were varied ($8\ \mu m \leq d \leq 120\ \mu m$, $0 \leq \delta \leq 1.7\ \mu m$). As aligning coatings, the polyimide CRC-6070X-1 from Sumitomo Chemicals was used.

In those experiments which require LCs with standard resistivities, mixture 3825 containing cyano compounds was used. The high resistivity experiments were performed with the TFT mixture 7380 whose polar components consist entirely of halogenated compounds; both are from F. Hoffmann-La Roche. The relevant physical properties of mixtures 3825 and 7380 are listed in Table I. Tetrabutylammoniumiodine (TBAI) served as an ionic dopant to adjust the specific resistivity of the LCs to the desired values.[1] Thus, it was possible to cover the broad range of specific LC-resistivity $10^6\ \Omega m \leq \rho_{LC} \leq 10^{12}\ \Omega m$.

TABLE I

Dielectric constants ($\varepsilon_{\parallel}$, $\varepsilon_{\perp}$, $\Delta\varepsilon$), bulk viscosity (η), melting temperature (T_m) and clearing temperature (T_c) of mixtures 3825 and 7380.

	$\varepsilon_{\parallel}$	$\varepsilon_{\perp}$	$\Delta\varepsilon$	η [cP]	T_m[°C]	T_c[°C]
3825	15.81	5.26	10.55	32.0	<-30	65.0
7380	8.55	3.73	4.82	16.5	<-30	78.8

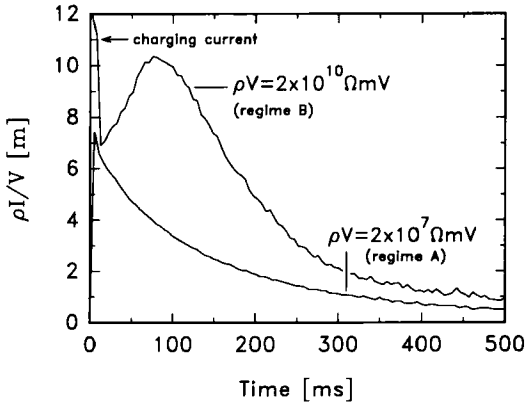

FIGURE 1 Normalized TN-LCD-currents in regimes A and B recorded at 22°C using mixtures 3825 (regime A) and 7380 (regime B). The respective driving voltages are 0.2 volts and 1.8 volts which are both below the mechanical thresholds of the mixtures.

3. EXISTENCE OF TWO DIFFERENT $\rho_{LC}V$-REGIMES A AND B

In our LCD experiments we found that distinctly different LCD current transients result when increasing either the specific LC-resistivity and/or the amplitude of the LCD driving voltage above a certain value of the product $\rho_{LC}V$. Figure 1 shows the different response of the normalized TN-LCD current I versus time upon polarity reversal of an applied voltage V_0 in the two regimes A [$\rho_{LC}(22°C) \cdot V < 10^9$ ΩmV] and B [$\rho_{LC}(22°C) \cdot V > 10^9$ ΩmV]. To avoid effects due to voltage-induced director deformations the driving voltages used in Figure 1 are below the mechanical thresholds of the LCs. In regime A a single exponential decay occurs whereas in regime B $I(t)$ exhibits a more complex behaviour (Figure 1) which others noted too.[4–6] Since it is the product $\rho_{LC}V$ which affects the time dependence $I(t)$, it follows from Figure 1 that great care has to be taken when determining ρ_{LCD} from $I(t)$-measurements; especially when investigating highly resistive LC-layers with large driving voltages. To avoid ambiguities when determining ρ_{LCD} and to remain in regime A, even when using highly resistive LCs, we therefore used small voltages $V_0 \leq 0.2\ V$ such that no current peak occurred. In this case and provided perfectly clean LCDs are used ρ_{LCD} is identical with ρ_{LC}; where ρ_{LC} follows from independent bulk resistivity measurements.

Like the time dependence of the LCD-current in Figure 1 also the decay of the

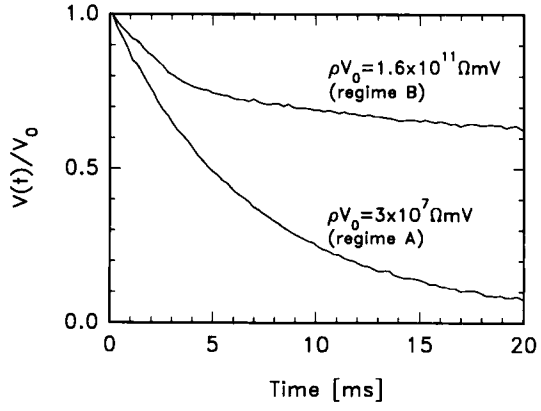

FIGURE 2 Time dependence of the voltage decay across a TFT-TN-LCD pixel in regime A and B upon disconnecting the voltage source V_0. Mixtures 3825 (in regime A) and 7380 (in regime B) were used for the measurements. Specific resistivities and measuring conditions: Regime A: $\rho(22°C) = 1.5 \times 10^8\ \Omega m$, $V_0 = 0.2$ V, $T = 22°C$; Regime B: $\rho(22°C) = 1.6 \times 10^{10}\ \Omega m$, $\rho(90°C) = 7 \times 10^8\ \Omega m$, $V_0 = 10$ V, $T = 90°C$. Different measuring temperatures were selected in the two regimes to allow the depiction of both measurements within the same time scale. The typical biexponential behaviour in regime B also holds at room temperature.

voltage $V(t)$ across an actively addressed TN-LCD, which is simulated by electronically disconnecting the TN-LCD from the driving voltage V_0, differs in the two regimes A and B. This is shown in Figure 2. From Figure 2 it follows that the ratio $V(t)/V_0$ obeys a single exponential decay in regime A. However, in regime B $V(t)/V_0$ is governed by a biexponential decay (Figure 2). Deviations from a single exponential decay are also reported in Reference 7. The ratio $V(t = 20\ ms)/V_0$ is a measure for the performance of an active matrix addressed LCD and for the TFT compatibility of the LC-material with respect to charge retention. $V(t = 20\ ms)/V_0 = 1$ if no voltage decay occurs during the frame time $t = 20$ ms.[3] Below we will show that the current- and voltage transient behaviour in regime B, which differs from that in regime A, is due to the formation of space charge which leads to inhomogeneous charge distribution within the LC-layer and to non-Ohmic resistivities ρ_{LC}.

4. REGIME A: $\rho_{LC}V < 10^9\ \Omega mV$

4.1. LCD-Equivalent Circuit in Regime A

In this paragraph it is shown that the complex impedance of TN- and STN-LCDs can be described in regime A by the linear equivalent circuit depicted in Figure 3. The LC-layer as well as the two polyimide aligning layers on the ITO electrodes are each represented by parallel RC-circuits. All circuit elements are assumed to be linear in regime A. Then, the single exponential current decay upon polarity

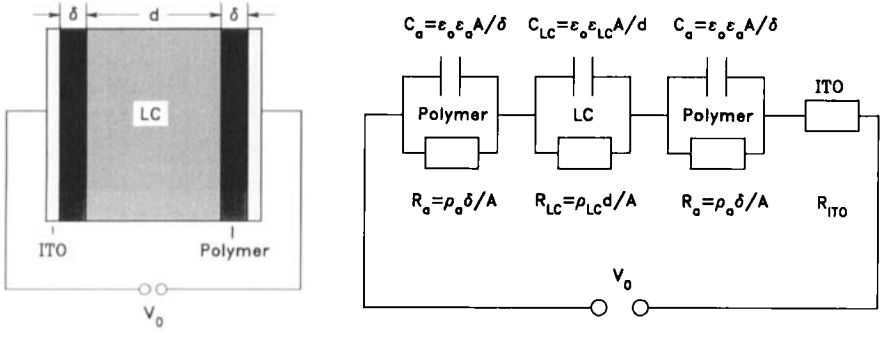

FIGURE 3 a) Schematic of a TN-cell; b) equivalent circuit of a TN-LCD.

reversal of the applied voltage V_0 in Figure 3 is governed by the time constant τ in Equation (1):

$$I(t) = I_\infty + I_0 \exp(-t/\tau), \quad \tau = \varepsilon_0 \frac{\frac{\varepsilon_a}{2\delta} + \frac{\varepsilon_{LC}}{d}}{\frac{1}{2\rho_a\delta} + \frac{1}{\rho_{LC}d}} \tag{1}$$

$$I_\infty = I(t = \infty) = V_0/(R_{LC} + 2R_a + R_{ITO}),$$

where ε_a, ε_{LC}, ρ_a, ρ_{LC} are the dielectric constants and the specific resistivities of aligning- and LC-layer respectively; ε_0 is the permittivity of vacuum.

To confirm the assumed linear equivalent circuit in regime A (Figure 3) the relevant LC- and LCD-parameters ρ_{LC}, d and δ were varied over wide ranges. Figures 4a–c show the experimental results and the calculated graphs. The graphs follow from Equation (1) and from $\rho_{LC} \ll \rho_a$ which holds in regime A. The results of Figures 4 confirm the dependences of the time constant τ on LC-resistivity ρ_{LC} (Figure 4a), cell gap d (Figure 4b) and aligning layer thickness δ (Figure 4c) which follow from Equation (1). Apart from the influence of ρ_{LC} on τ (Figure 4) it is interesting to note the strong influence of the LCD parameters d and δ on τ in Figure 4. Especially the strong decay of τ with increasing aligning layer thickness δ is noteworthy (Figure 4c).

LCDs with different aligning layer thicknesses $\delta < 50$ nm have been prepared. Unfortunately, the accuracy with which δ was determined (with an interference microscope) decreases with decreasing layer thickness. However, qualitatively relation (1) also holds for $\delta < 50$ nm.

From Equation (1) follows for the voltage V_{LC} across the LC-layer for $t \to \infty$ in regime A:

$$V_{LC}(t = \infty) = V_0 \frac{R_{LC}}{R_{LC} + 2R_a + R_{Ito}} \tag{2}$$

Because usually $R_{LC} \ll R_a$ holds, V_{LC} $(t \to \infty)$ in Equation (2) becomes small,

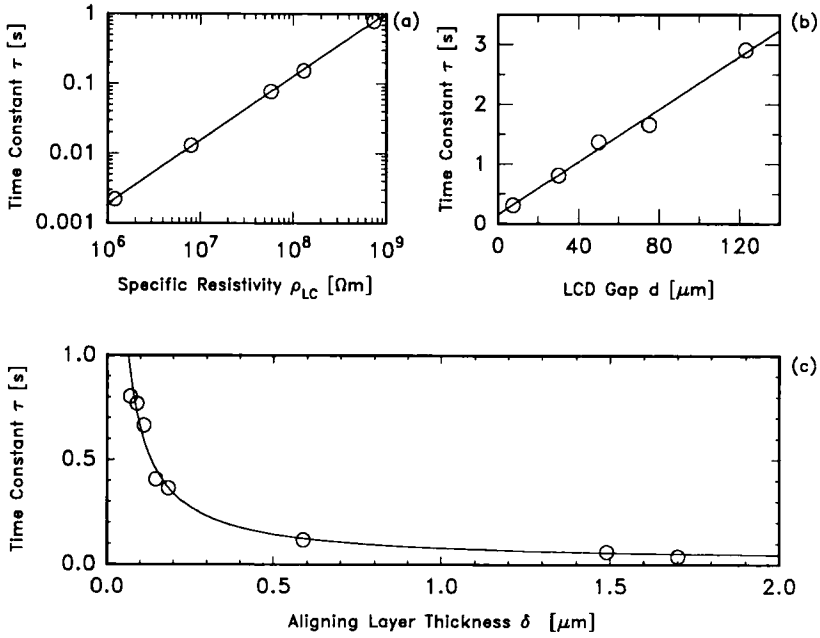

FIGURE 4 Dependence of the time constant τ on ρ_{LC}, d and δ. V_0 = 0.2 V; LC-mixture TN-3825 from F. Hoffmann-La Roche, doped with TBAI for adjustment of ρ_{LC}. a) d = 8 μm; δ = 0.15 μm; b) ρ_{LC} = 1.4 × 10^6 Ωm; c) d = 10 μm, ρ_{LC} = 2.5 × 10^8 Ωm.

thus causing the nematic director to relax. This leads to a decrease of the LCD transmission with time.

Like Equation (1) also Equation (2) follows from the assumption that the equivalent LCD-circuit in Figure 3 is linear in regime A. That is, all resistivities in Equations (1 and 2) are Ohmic. However, linearity holds only as long as the charge carrier density ($\propto 1/\rho_{LC}$) in the LC-layer is essentially constant. If, for instance at high voltages, a depletion of charge carriers ($\propto V$) in the bulk of the LC-layer occurs, which will be shown in §5 to happen in regime B, the charge distribution in the LCD becomes inhomogeneous. This leads to a build-up of space charge at the LCD electrodes rendering the linear equivalent circuit in Figure 3 and Equations (1) and (2) invalid.

4.2. Frequency Dependence of the Optical LCD-Threshold Voltage in Regime A

From the complex LCD impedance of the linear equivalent circuit in Figure 3, which was shown in §4.1 to be valid in regime A, follows that the actual rms voltage V_{LC} across the LC-layer must depend on frequency:

$$V_{LC}(f) = \sqrt{\frac{R_{LC}^2 ab^2 V_0^2}{[2R_a a + R_{LC} b + R_{Ito} ab]^2 + \omega^2 [2R_a^2 C_a a + R_{LC}^2 C_{LC} b]^2}}, \qquad (3)$$

where

$$a = 1 + (\omega R_{LC} C_{LC})^2; \qquad b = 1 + (\omega R_a C_a)^2; \qquad \omega = 2\pi f.$$

As a consequence also the voltage-induced deformation of the nematic director in the LCD and therefore its electro-optical signal must depend on frequency and on the circuit parameters depicted in Figure 3.

Apart from the voltage-induced director deformation which governs the electro-optical performance of field-effect LCDs Gruler and Cheung showed that the LC-conductivity σ may also contribute to the director deformation and thus affect the electro-optics. For the voltage $V_{LC}(\phi)$ required to induce a director deformation ϕ_m in the center of a conducting, parallel aligned LC-layer they derived[8]:

$$V_{LC}(\phi) \cong (1 + \phi_m^2(k_{33}/k_{11} + c)/4)V_{th}, \tag{4}$$

where

$$c = \frac{\dfrac{\sigma_\parallel - \sigma_\perp}{\sigma_\perp} + \left(\dfrac{\omega}{\omega_0}\right)^2 \dfrac{\varepsilon_\parallel - \varepsilon_\perp}{\varepsilon_\perp}}{1 + (\omega/\omega_0)^2}; \qquad \omega_0 = \frac{\sigma_\perp}{\varepsilon_0 \varepsilon_\perp} \quad \text{and} \quad \omega = 2\pi f.$$

k_{11} and k_{33} are the splay and bend elastic constants, $\Delta\varepsilon = (\varepsilon_\parallel - \varepsilon_\perp)$ is the static dielectric anisotropy and V_{th} the threshold voltage for mechanical deformation of the LC-layer. For highly resistive LCs where $\sigma = 0$, Equation (4) reduces to the purely field-induced case for which the current-induced frequency dependence disappears.

Because the frequency dependent coefficient c in Equation (4) does not depend on elastic properties, the dependency $V_{LC}(\phi)$ of a parallel LCD on frequency should be the same as $V_{LC}(\phi)$ of a TN-LCD. However, since the elastic constants affect the maximal change of $V_{LC}(\phi)$ with frequency the dynamic range of $V_{LC}(\phi)$ of a TN-LCD is only partly described by Equation (4). Despite this restriction it is interesting to estimate the combined influence of conductivity-induced and equiv-

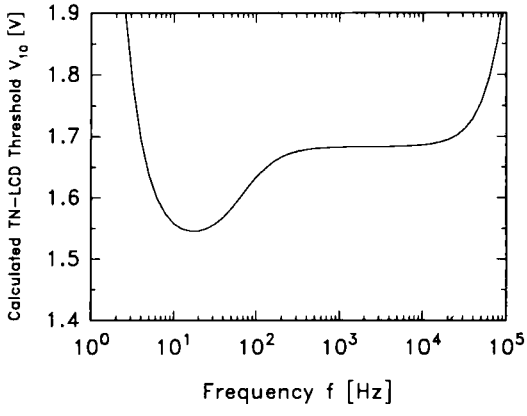

FIGURE 5 Calculated frequency dependence $V_{10}(f)$ of the optical TN-LCD threshold voltage. LC-material parameters of mixture 3825: $\rho_{LC} = 5 \times 10^7$ Ωm, $\varepsilon_\perp$(LC) = 5.3, $\Delta\varepsilon$(LC) = 10.5, $\varepsilon_a = 3$, $\sigma_\parallel/\sigma_\perp = 1.3$, $k_{33}/k_{11} = 1.5$, $\phi_m = 30°$, Vth = 1.32. LCD-parameters: $\rho_a = 10^{10}$ Ωm, $R_{10} = 5$ kΩ, $d = 8$ μm, $\delta = 0.1$ μm.

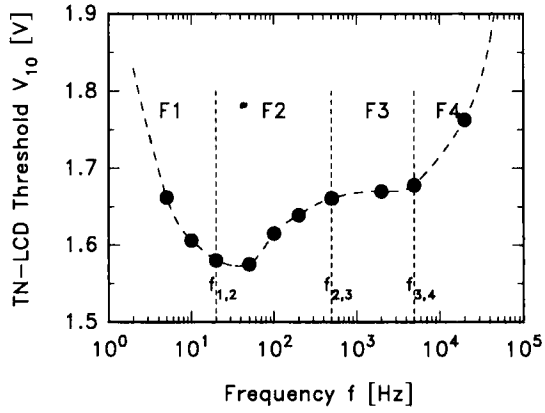

FIGURE 6 Frequency dependence of the optical TN-LCD threshold voltage V_{10} at room temperature; mixture: 3825; $\rho_{LC} = 5 \times 10^7$ Ωm; $\delta = 0.15$ μm, $d = 8$ μm; square wave drive.

alent circuit-induced frequency dependence on the optical TN-LCD threshold voltage. If one inserts for the angle of director deformation the angle ϕ_m that corresponds with 10% TN-LCD transmission, the voltage V_0 which has to be applied to the LCD follows from the equality of Equations (3) and (4). In this case V_0 is identical with the optical TN-LCD threshold voltage $V_{10}(f)$. Figure 5 shows the calculated frequency dependence $V_{10}(f)$ for a TN-LCD. A similar dependence holds for STN-LCDs. The calculation is based on the LC- and display parameters depicted in the caption of Figure 5. The calculated frequency dependence of V_{10} depicted in Figure 5 which follows from the equivalent circuit of Figure 3 and from Equation (3) is experimentally confirmed in the following.

Figure 6 shows the measured frequency dependence $V_{10}(f)$ of a TN-LCD comprising mixture 3825 ($\rho_{LC} = 5 \times 10^7$ Ωm). Specific resistivities of modern LC-mixtures for TN- and STN-LCDs usually exceed 10^9 Ωm. However, mixtures with low threshold voltages which contain highly polar cyano compounds are very sensitive to ion contamination during the LCD filling process. In these cases, values of $\rho_{LCD} < 10^8$ Ωm are often realistic. In Figure 6 the following four frequency ranges are distinguished: F1($f \leq 20$ Hz), F2 (20 Hz $< f \leq 500$ Hz), F3 (500 Hz $< f \leq 5$ kHz) and F4($f > 5$ kHz).

Frequency range F1: The dependence of $V_{10}(f)$ of the TN-threshold voltage at low frequencies is determined by the LC-resistivity ρ_{LC}, the LCD spacing d and the thickness δ of the aligning layer (Figure 3). Qualitatively V_{10} (F1) agrees with the equivalent circuit of Figure 3 and equation (3). The latter predicts a decrease of $V_{LC}(f)$ with decreasing frequency in range F1. Therefore, the external LCD driving voltage V_0 has to increase with decreasing frequency to maintain a constant (10%) transmission of the LCD (Figures 5 and 6). Since it is the time constant τ in Equation (1) which governs the onset of the increase of $V_{10}(f)$ in range F1, the frequency range F1 shifts towards lower frequencies for increasing ρ_{LC} and/or for decreasing δ. That is, the border frequency $f_{1,2}$ decreases (Figure 6).

Frequency range F2: The border frequency $f_{2,3}$ at which the decrease of $V_{10}(f)$ starts in Figure 6 (Figure 5) shifts towards lower values with increasing LC-resistivity ρ_{LC}. The decrease is neither affected by the LCD gap d nor by the thickness δ of

the aligning layers. The decrease cannot be explained by the frequency dependency of the equivalent circuit postulated in Figure 3 unless one assumes current-induced director deformations to occur in the LC-layer at $f_{2,3}$ (Equation 4). Indeed, the decrease of $V_{10}(f)$ at $f_{2,3}$ corresponds well with the current-induced deformation mechanism discussed above: The decrease depends on magnitude and anisotropy of the LC-resistivity ρ_{LC} and on the dielectric constant(s) ε_{LC}. In agreement with Equation (4) decreasing $\Delta\rho_{LC}$ and/or increasing $\Delta\varepsilon_{LC}$ cause V_{10} to decrease.

Frequency range F3: Within range F3 the threshold voltage V_{10} is, as required for proper LCD-operation, frequency independent (Figure 6). Again, this experimental result qualitatively agrees with the calculated dependence depicted in Figure 5. The frequency independence follows from the equivalent circuit of Figure 3 and from Equation (3) from which the effective voltage V_{LC} across the LC-layer in F3 becomes:

$$V_{LC} = \frac{C_a}{C_a + 2C_{LC}} V_0 = \frac{\varepsilon_a d}{\varepsilon_a d + 2\varepsilon_{LC}\delta} V_0 \tag{5}$$

From Equation (5) follows $V_{LC} = V_0$ for $\varepsilon_a d >> 2\,\varepsilon_{LC}\delta$. Thus, in F3 V_{10} depends only on the elastic, dielectric and optical LC-material parameters.[9] For highly resistive LC-materials ($\rho_{LC} > 10^{10}\,\Omega$m) the frequency independent range F3 extends below 10 Hz, thus broadening the range within which an LCD can be operated without cross-talk.

In this context it should be noted that TN-LCDs with very low threshold voltages ($V_{10} \lesssim 1$ volt) comprise LCs with large dielectric anisotropies $\Delta\varepsilon$. Therefore, and because an appreciable field-induced parallel director alignment exists already at V_{10} in a TN-LCD,[9] the above condition $\varepsilon_a d >> 2\varepsilon_{LC}\delta \sim 2\varepsilon_{\parallel}\delta$ may no longer hold. Thus, for large $\Delta\varepsilon$'s a rather strong influence of the aligning layer thickness δ on the optical threshold V_{10} results which causes the V_{10}-plateau in range F3 of Figures 5 and 6 to increase with increasing δ (Equation 5).

Frequency range F4: From Figure 3 and Equation (3) follows an increasing voltage decay across the ITO-series resistance R_{ITO} with increasing frequency in range F4. This leads to an increase of the LCD threshold voltage V_{10} with increasing frequency (to maintain a constant optical transmission of 10%). The experiments in Figure 6 confirm the calculated frequency dependence $V_{10}(f)$ depicted in Figure 5. Reducing R_{ITO} shifts the border frequency $f_{3,4}$ upwards, thus extending the frequency independent, cross-talk free LCD-operating range F3 towards higher frequencies.

Apart from the LCD technology-dependent increase of V_{10} in range F4, dielectric dispersion in the LC-material may also contribute to the increase of V_{10} at high frequencies in range F4.[1] However, since modern LC-materials which are designed for high information content LCDs do not comprise molecules with strong rotational hindrance around their short axes, dielectric dispersion does not occur below 100 kHz in the LCs used here.

5. REGIME B: $\rho_{LC}V > 10^9\ \Omega$mV

In regime B where $\rho_{LC}V > 10^9\ \Omega$mV holds, the LCD current transient response is distinctly different from that in regime A (§3). The different response indicates

that the linearity of the LCD equivalent circuit in Figure 3 is no longer valid in regime B. In the following the causes for the nonlinearities of the circuit elements in regime B are discussed and it is shown how they affect the performance of LCDs comprising highly resistive LC-materials, that is, active matrix addressed LCDs. To exclude ambiguities due to field-induced director reorientation, most of the following experiments were performed in the isotropic phase of LC-mixture 7380.

The undoped TFT-TN-mixture 7380 exhibits a specific resistivity $\rho_{LC} = 10^{12}\ \Omega m$ at room temperature. Because of this large resistivity the transient current experiments are very difficult to perform. Therefore, all of the following experiments were made with a slightly more conductive version of 7380 ($\rho_{LC} = 1.6 \times 10^{10}\ \Omega m$).

5.1. Holding Ratios and LCD Driving Conditions

Figure 7 shows the time dependence of the normalized voltage decay $V(t)/V_0$ across the TN-LCD upon application of a short (64 μs) pulse of amplitude V_0 via a high

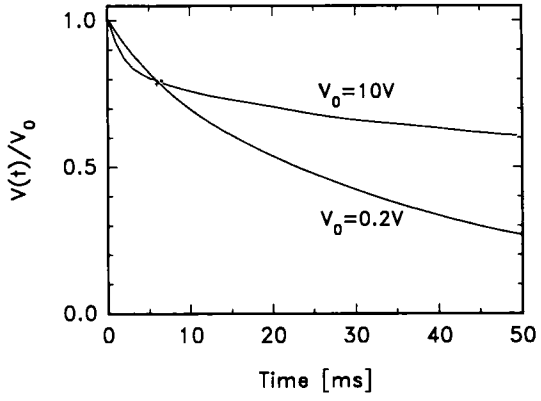

FIGURE 7 Normalized voltage $V(t)/V_0$ across a LCD-Pixel upon disconnecting different driving voltages V_0; measurements made at $T = 90°C > T_c = 79°C$.

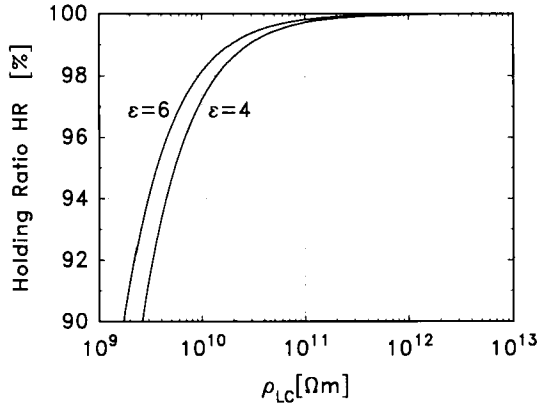

FIGURE 8 Calculated dependence of the LCD holding ratio HR (Equation 6) on LC-resistivity ρ_{LC}. A single exponential decay $V(t)$ is assumed in the calculation; i.e. the equivalent circuit of Figure 3 is assumed to hold.

impedance FET to the LCD.[3] After each frame time (t = 50 ms) the sign of V_0 is reversed. $V(t)/V_0$ scales with the voltage holding ratio HR of the LCD pixel.[3] From Figure 7 follows that for different amplitudes of V_0 quite different decays result. The decay time constant at low voltages (V_0 = 0.2 volts) in Figure 7 is the same as the time constant $R_{LC}C_{LC}$ in Figure 3. Thus, the specific LC-resistivity ρ_{LC} which follows from the voltage decay $V(t)/V_0$ at low driving voltages is identical with the specific resistivity $\rho_{LCD} \leq \rho_{LC}$. However, contrary to the small signal response, the decay of $V(t)/V_0$ at large driving voltages V_0 becomes biexponential (Figure 7). This shows that great care has to be taken when determining specific LC-resistivities ρ_{LC} from voltage holding ratio experiments.

From Figure 7 and from the definition of the holding ratio HR by Equation (6)[3] follows that HR which characterizes the charge retention of an active matrix addressed LCD-pixel depends on LCD driving voltage.

$$HR = \frac{V(T)_{rms}}{V_0} \cdot 100 = \frac{1}{V_0}\left(\frac{1}{T}\int_{t=0}^{T} V^2(t)\,dt\right)^{1/2} \cdot 100 \quad [\%], \quad T = 20 \text{ ms} \quad (6)$$

Thus, the much larger holding ratio which result for voltages $V_0 >> 0.2$ volts in Figure 7 cannot be explained by the conventional RC-time constant of the LC-layer.

In the holding ratio context and under the assumption that the linear equivalent circuit of Figure 3 is applicable it is interesting to note the dependence of HR on ρ_{LC} which follows from Equation (6). For two different liquid crystals with the respective dielectric constants ε = 4 and ε = 6, Figure 8 shows the calculated dependence HR (ρ_{LC}). From the strongly nonlinear dependence in Figure 8 it follows that the maximum holding ratio $HR \simeq 100\%$ = constant is achieved for $\rho_{LC} \gtrsim 10^{12}$ Ωm. Increasing ρ_{LC} further does no longer affect HR.

Because the linearity of the LCD equivalent circuit in Figure 3 does not hold in regime B, the question arises whether the decay voltage $V(t)$ in holding ratio experiments is identical with the voltage across the LC-layer. This was investigated by determining in a first experiment the optical TN-LCD transmission simultaneously with the voltage decay $V(t)$. $V(t)$ was then transferred to a programmable function generator which served in a second experiment as the voltage source to (continuously) drive the LCD. The upper part of Figure 9 shows the time response of the TN-LCD transmission in the two experiments (graphs a and b). The bottom shows the corresponding time response $V(t)$ of holding ratio experiment 1. $V(t)$ at the bottom of Figure 9 is identical with the synthesized LCD-driving voltage applied to the LCD in experiment 2. From the virtually identical time responses of the transmissions in Figure 8 (graphs a and b) follows that the decay voltage $V(t)$ determined in holding ratio experiments is indeed the effective voltage across the LC layer in the LCD.

5.2. Charge Carrier Transport Mechanism in Regime B

To identify the cause which leads to the biexponential voltage decay in LCD holding ratio experiments where large driving voltages and/or large LC-resistivities are

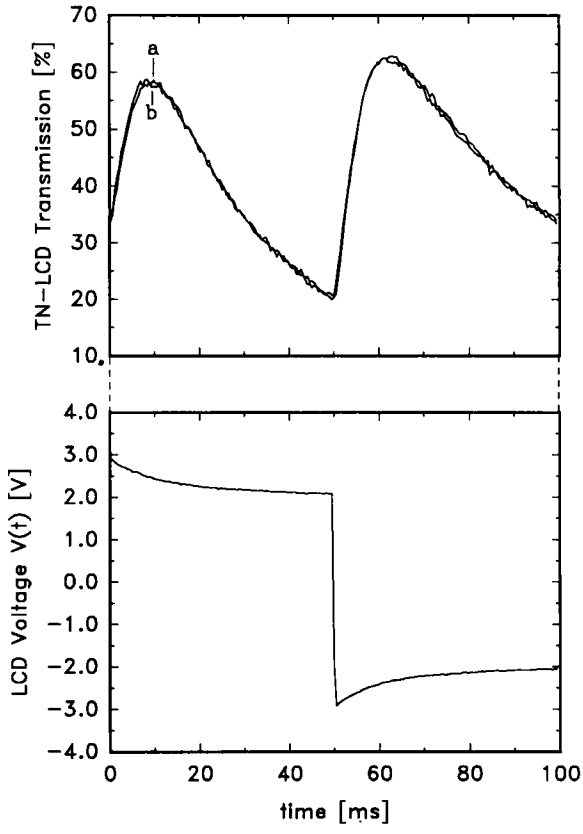

FIGURE 9 Upper part: time response of the TN-LCD transmission in a holding ratio experiment (graph a) and upon directly addressing the LCD with the voltage $V(t)$ (graph b). Lower part: time dependence of the LCD voltage $V(t)$ which follows from the holding ratio experiment and which corresponds with the above graph a. The synthesized voltage used to continuously drive the LCD and which leads to the above graph b has the same shape as $V(t)$. (V_0 = 3 volts, frame time t = 50 ms, T = 70°C, d = 8.3 μm, mixture 7380).

involved (i.e. in regime B) the above LCD-voltage decay measurements (Figure 7) were performed with different amplitudes V_0. The results depicted in Figure 10 show the transition from the single exponential voltage decay $V(t)$ at low driving voltages to the biexponential decay at higher voltages. Figure 10 also shows that the amplitude of the initial fast voltage decay in the biexponential regime is constant for $V_0 \gtrsim 4$ volts while its time constant τ_1 decreases with increasing V_0. The experiments in Figure 10 were made in the isotropic phase of the LC-material. However, the same results are obtained in the nematic state. This proves that effects due to field-induced director realignment are of second order in this context. The constant amplitude ΔV_1 of the initial fast decay $V(t)$ for $V_0 \geq 4$ volts indicates that $Q_1 = C\Delta V_1$ is the total charge of the high mobility ions in the LC-layer; where C is the pixel capacitance. Since the measurements are made in the isotropic phase, C = constant.

To actually determine the charge Q_1 which gives rise to the initial fast voltage decay τ_1 in Figure 10 and to check its dependence on driving voltage V_0 the LCD-

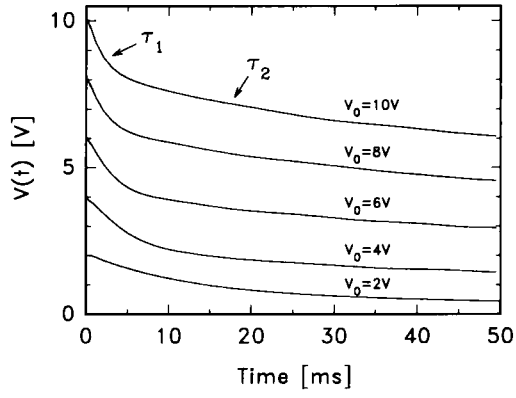

FIGURE 10 Biexponential LCD-voltage decay upon disconnecting (different) driving voltages V_0 at $t = 0$; $T = 90°C > T_c$.

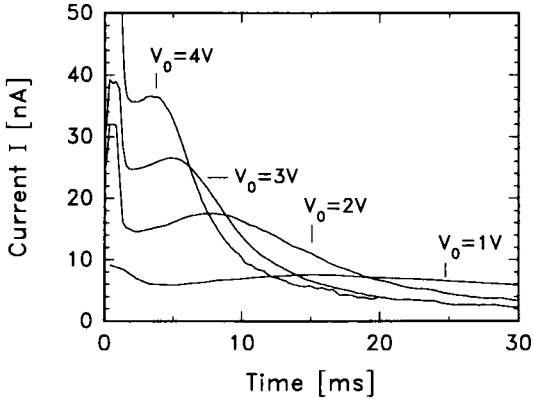

FIGURE 11 LCD current transients for different V_0; $T = 90°C > T_c$.

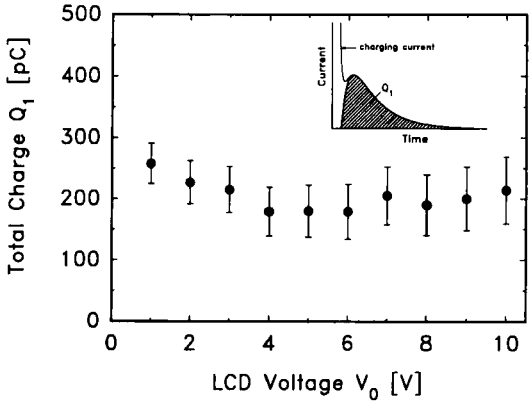

FIGURE 12 $Q_1 = \int I\,dt$ calculated from the measurements in Figure 11.

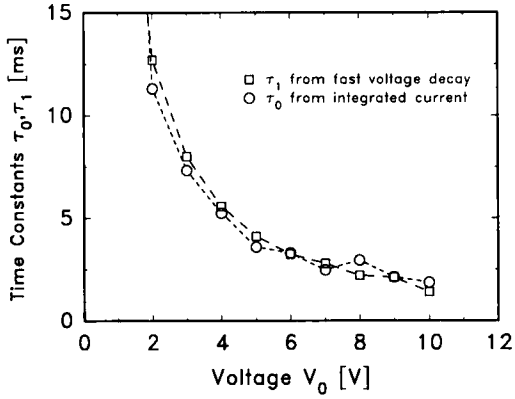

FIGURE 13 Voltage decay time constant τ_1 and current response time constant τ_0 versus LCD-driving voltage V_0. τ_1 follows from Figure 10 and τ_0 from Figure 11 and Equation (7); $T = 90°C > T_c$; mixture 7380.

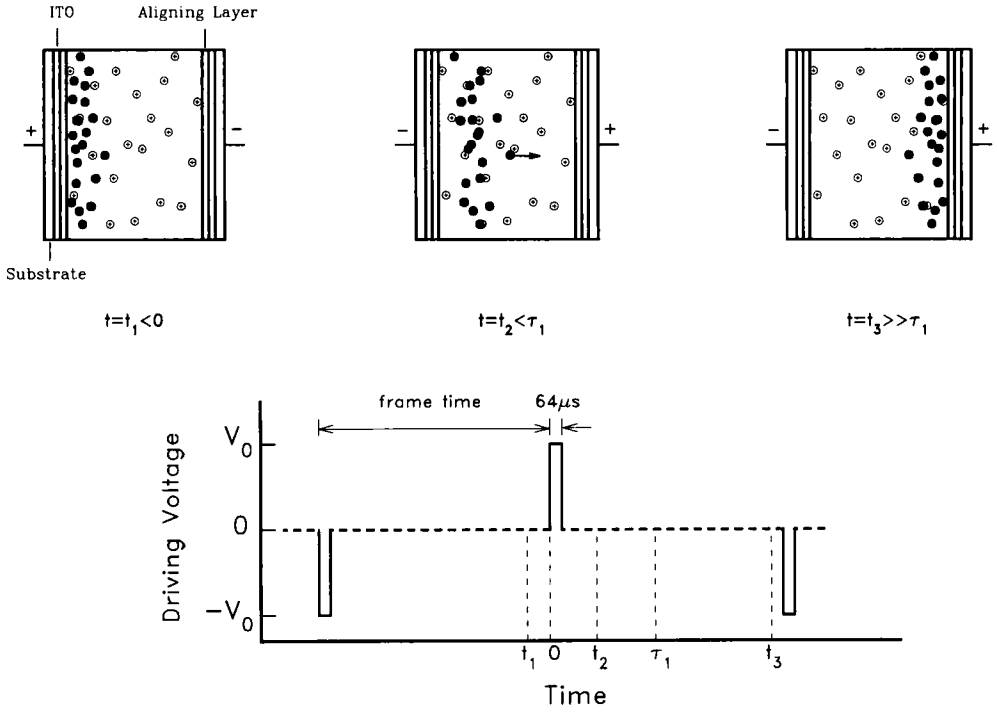

FIGURE 14 Upper part: Time dependent build-up of space charge in the LCD in regime B due to high mobility residual ions. The low mobility (positive) counter ions are assumed to be stationary within the time frame (lower part) of the LCD-driving scheme.

current transients versus V_0 were recorded. The results are depicted in Figure 11. Although a strong dependence of the position of the current peak on applied voltage follows from Figure 10, the integrated peak current $Q_1 = \int I_{\text{Peak}}\, dt$ is nearly constant for $0.2 \leq V_0 \leq 10$ V. This is shown in Figure 12. Moreover, Q_1 does hardly depend

on temperature between 20°C and 120°C. The voltage ΔV_1 which follows from $\Delta V_1 = Q_1/C$ in Figure 12 agrees quite well with the constant amplitude of the fast voltage decay of Figure 10. Moreover, the time τ_0 which follows from the current response of Figure 11 and from

$$Q(\tau_0) = \int_0^{\tau_0} I_{\text{peak}}\, dt = (1 - 1/e)Q_1 \tag{7}$$

is identical with the fast voltage decay time constant τ_1 (Figure 10); where $V(\tau_1) = (1 - 1/e)\Delta V_1$ holds. The identical time constants τ_1 and τ_0 which follow from Figures 10 and 11 are depicted in Figure 13. We therefore conclude that the fast initial voltage decay in Figure 10 and the current transients in Figure 11 are caused by the same transport mechanism. That is, by rather mobil residual ions whose low concentration in the LC-layer gets inhomogeneously distributed across the layer upon application of V_0. Because of their high mobility (current transients) the inhomogeneities occur within milliseconds. This leads to space charge effects and to nonlinearities in the LCD-equivalent circuit of Figure 3. From LCD current-transient measurements made at room temperature the mobility of the fast ions $\mu = 6 \times 10^{-6}$ cm²/Vs was determined. This value agrees well with $\mu = 4.7 \times 10^{-6}$ cm²/Vs of the ion mobilities in LCs reported earlier under different experimental conditions.[1]

Because of space charge effects in regime B the charge carriers are mainly located at the boundary layers of the LCD. This is schematically shown in Figure 14. Upon polarity reversal of the applied voltage the fast ions move towards the opposite electrode which leads to the increase of the initial current in Figure 11. As soon as the ion front arrives at the respective aligning layer the current decreases again.

The cause for the slow voltage decay τ_2 in Figure 10 is not yet understood. Because of the extremely small associated LCD-current it is difficult to correlate charge-transport phenomena with τ_2. However, one possible cause is the slow transport of bulky counter ions in the LC-layer.

From the above it follows that amplitude and shape of the current peak as well as the fast voltage decay in charge retention experiments are strongly affected by the amount and by the species of residual ionic impurities in the LC-material. While the amount of field-displaced carriers is negligible in regime A compared with the total number of free carriers, the same field-induced separation of ions leads to a nonuniform charge distribution in the LC-layer in regime B. As a consequence, the specific resistivity ρ_{LC} becomes time dependent in regime B.

6. CONCLUSIONS

Correlations are shown between display- and LC-material parameters and the performance of passively and actively matrix addressed TN-LCDs. The time- and frequency dependence of the electro-optical performance of LCDs on LC-resistivity, dielectric constants, LCD cell gap, electrode resistivity and aligning layer thickness are modelled by means of an electrical equivalent circuit. Apart from field-induced

director deformations, LC-conductivity-induced deformations are taken into account. From the model follows the time- and frequency dependency of the electro-optical performance of TN-LCDs as well as their current- and voltage transient response. The circuit elements are shown to be linear in regime A, where $\rho_{LC}V < 10^9\,\Omega$mV holds; whereas nonlinear space charge effects strongly influence the LCD-performance in regime B ($\rho_{LC}V > 10^9\,\Omega$mV).

The frequency dependence of the optical threshold voltage of TN- and STN-LCDs between dc and 100 kHz follows from the proposed model. By properly selecting LC- and -LCD parameters the frequency independent operating range of LCDs can be extended. This simultaneously extends the cross-talk free frequency range of LCD operation.

The holding ratio of TFT-TN-LCDs is shown to be strongly influenced by the amplitude of the first of two exponential voltage decay functions which occur in regime B. The fast voltage decay is shown to be correlated with the current peak which is due to the space-charge limited conductivity conditions in regime B. A nonuniform charge distribution in the LCD caused by the field-induced separation of the limited number of charge carriers in the LC-layer is the reason for both, the fast initial voltage decay and the current peak. The mobilities which follow from the current transients in regime B for the (small) high mobility ions are in good agreement with the ion mobilities determined previously. The cause for the slow voltage decay in regime B is not yet understood. It may be due to low mobility (bulky) counter ions.

References

1. M. Schadt and C.v. Planta, *J. Chem. Phys.*, **63**, 4379 (1975).
2. H. Seiberle and M. Schadt, *Digest SID 92*, 25, 1992.
3. F. Moia and M. Schadt, *Proc. SID 32, No. 4*, 361 (1991).
4. A. Mochizuki, T. Yoshihara, K. Motoyoshi and S. Kobayashi, *Jpn. J. Appl. Phys.*, **29**, L322 (1990).
5. A. Sugimura, Y. Takahashi, H. Sonomura, H. Naito and M. Okuda, *Mol. Cryst. & Liq. Cryst.*, **180B**, 313 (1990).
6. B. Maximus, P. Vetter and H. Pauwels, *Digest SID 91*, 53 (1991).
7. K. H. Yang, *J. Appl. Phys.*, **67**, 36 (1990).
8. H. Gruler and L. Cheung, *J. Appl. Phys.*, **46**, 5097 (1975).
9. M. Schadt and P. Gerber, *Zeitschr. Naturforsch.*, **37a**, 165 (1982).